BIOCHEMISTRY
including biophysical chemistry & molecular biology

ARTICLE

pubs.acs.org/biochemistry

Using Fluorine Nuclear Magnetic Resonance To Probe Changes in the Structure and Dynamics of Membrane-Active Peptides Interacting with Lipid Bilayers

Yuta Suzuki,[†] Benjamin C. Buer,[†] Hashim M. Al-Hashimi,[†,§] and E. Neil G. Marsh[*,†,§,‡]

[†]Department of Chemistry, [‡]Department of Biological Chemistry, and [§]Department of Biophysics, University of Michigan, Ann Arbor, Michigan 48109, United States

Supporting Information

ABSTRACT: The antimicrobial peptide MSI-78 serves as a model system for studying interactions of bioactive peptides with membranes. Using a series of MSI-78 peptides that incorporate L-4,4,4-trifluoroethylglycine, a small and sensitive ^{19}F nuclear magnetic resonance probe, we investigated how the local structure and dynamics of the peptide change when it binds to the lipid bilayer. The fluorinated MSI-78 analogues exhibited position-specific changes in ^{19}F chemical shift ranging from 1.28 to −1.35 ppm upon binding to lipid bicelles. The largest upfield shifts are associated with the most hydrophobic positions in the peptide. Changes in solvent isotope effects (H_2O/D_2O) on ^{19}F chemical shifts were observed for the peptides that are consistent with the MSI-78 solvent-inaccessible hydrophobic core upon binding bicelles. Transverse relaxation measurements of the ^{19}F nucleus, using the Carr−Purcell−Meiboom−Gill pulse sequence, were used to examine changes in the local mobility of MSI-78 that occur upon binding to the lipid bilayer. Positions in the hydrophobic core of peptide−membrane complex show the greatest decrease in mobility upon binding of the lipid bilayer, whereas residues that interact with lipid headgroups are more mobile. The most mobile positions are at the N- and C-termini of the peptide. These results provide support for the proposed mechanism of membrane disruption by MSI-78 and reveal new details about the dynamic changes that accompany membrane binding.

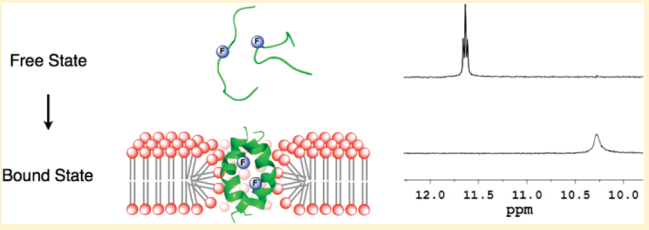

The interaction of small peptides with the lipid bilayer of the cell membrane is important in a variety of biological processes.[1−6] These membrane-active peptides may have protective properties like antimicrobial peptides (AMPs), anticancer peptides, and antiviral peptides or be involved in pathological processes with peptides such as cell-penetrating peptides, viral fusion peptides, and venom peptides. For all these classes of peptides, interactions between the membrane lipid bilayer and the peptide are central to their biological functions.

Characterizing peptide−membrane interactions is often challenging because of the transient and dynamic nature of these interactions. The peptide may adopt different orientations with respect to the lipid bilayer and different oligomerization states that are concentration-dependent. Solid-state nuclear magnetic resonance (NMR) experiments have used various NMR-active nuclei to investigate the structures and orientations of AMPs bound to lipid membranes.[7−12] These include studies using fluorine-labeled AMPs to provide information about peptide orientation in membranes.[13−15] However, these experiments require peptide concentrations that are orders of magnitude higher than their physiologically active range, so it is not always clear whether such structures represent biologically active species. Solution-phase fluorine NMR has proven to be an informative tool for investigating biological interactions, for example, in probing the dynamics of soluble proteins[16−18] and the immersion depth of lipophilic molecules in lipid bilayers.[19,20]

AMPs make up a diverse family of membrane-active peptides found in essentially all multicellular organisms. Although some AMPs have specific intracellular targets,[1] most exert their antimicrobial activity by binding directly to the microbial membrane and compromising its integrity.[21−23] Almost all AMPs are highly amphipathic, with one face of the peptide being hydrophobic and the other face presenting a cluster of positively charged residues.[24−26] The selectivity of AMPs for bacterial membranes arises primarily from electrostatic interactions between the positively charged peptide and the negatively charged phospholipids that predominate in bacterial cell membranes. Eukaryotic membranes, which contain predominantly neutral phospholipids, are usually less susceptible to disruption by AMPs; the presence of cholesterol in eukaryotic membranes also helps prevent the disruption of membranes by AMPs.[27] Upon association with the membrane, disruption of the bacterial membrane may proceed through a number of mechanisms, including the formation of pores, membrane thinning, and detergent-like action.[23,28,29]

Received: April 26, 2011
Revised: June 3, 2011
Published: June 06, 2011

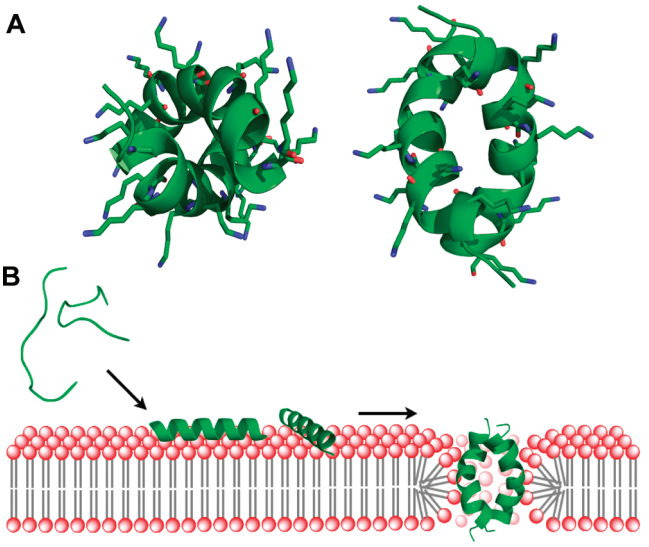

Figure 1. (A) Two views of the structure of MSI-78, determined from NMR experiments,[31] with peripheral lysine residues shown as sticks. (B) Cartoon illustrating the mechanism for insertion of MSI-78 into a lipid bilayer to form toroidal pores.

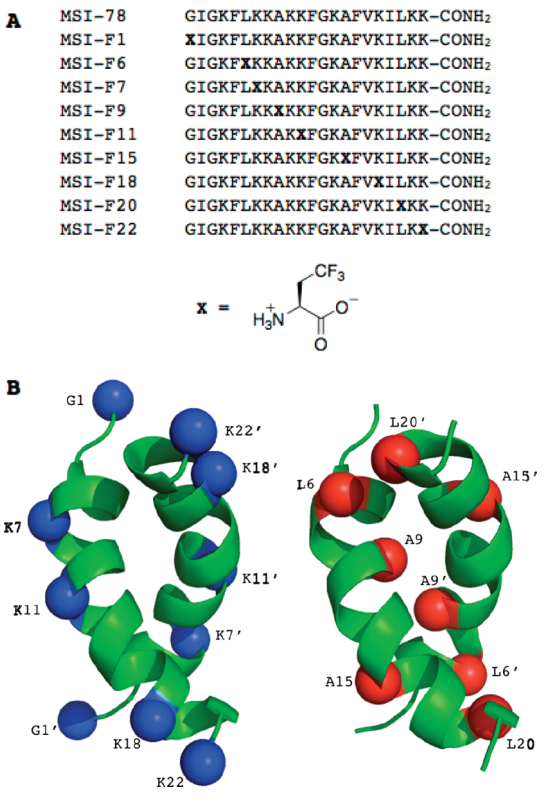

Figure 2. (A) Primary sequence of MSI-78 and the sequences of TfeG-substituted peptides used in this study. (B) Positions of amino acid substitutions mapped onto the structure of the MSI-78 dimer formed in DPC micelles. Substitutions at hydrophilic positions (blue spheres) are shown on the left; substitutions at hydrophobic positions (red spheres) are shown on the right.

Our studies have focused on the potent, synthetic AMP, MSI-78 (pexiganan), which provides a convenient model system for investigating peptide−membrane interactions. MSI-78 is thought to disrupt bacterial membranes by forming toroidal pores in the lipid bilayer,[30] as illustrated in Figure 1. On the basis of a combination of solution and solid-state NMR experiments, the peptide has been shown to adopt a dimeric α-helical coiled coil structure (Figure 1) in the presence of 3:1 POPC/POPG liposomes.[31] The dimer interface is formed by contacts between hydrophobic residues, whereas the positively charged lysine residues face the exterior of the structure and interact with hydrophilic lipid headgroups.

In previous studies, our group and others[32−36] have demonstrated that the incorporation of fluorinated amino acids into AMPs is an effective strategy for modulating their biological properties and can be used to study AMP−membrane interactions. For example, we showed that incorporating hexafluoroleucine at four positions in the α-helical AMP MSI-78 resulted in increased potency toward some bacterial strains and protection against proteolysis when bound to lipid vesicles.[32]

Recently, we turned our attention to using fluorine-containing peptides to probe the interaction of AMPs with membranes by exploiting the sensitive NMR properties of the ^{19}F nucleus. We demonstrated that binding of MSI-78 to small unilamellar vesicles and bicelles could easily be detected by following changes in the ^{19}F chemical shifts of MSI-78 variants containing L-4,4,4-trifluoroethylglycine (TfeG).[37] We also showed that the local dynamical properties of the membrane-bound peptide in the vicinity of the label could be investigated by measuring the transverse relaxation rate (R_2) of the ^{19}F nucleus using CPMG relaxation dispersion experiments. Here we have extended these measurements to examine the dynamics of the MSI-78−membrane complex by incorporating CF_3 probes at strategic positions throughout the peptide and measuring the associated changes in chemical shifts, solvent isotope effects on chemical shifts, and changes in R_1 and R_2 values.

EXPERIMENTAL PROCEDURES

Peptide Synthesis. Racemic 4,4,4-trifluoroethylglycine (TfeG) was purchased from SynQuest Laboratories and enzymatically resolved (porcine kidney acylase I), resulting in L-4,4,4-trifluoroethylglycine having a >99% enantiomeric excess.[38] The pure amino acid was converted to its t-Boc derivative by standard procedures. The sequences of MSI-78 derivatives are shown in Figure 2. Peptides were synthesized manually by either standard t-Boc procedures on MBHA resin or f-moc procedures on PAL-PEG resin, as described previously.[39,40] Peptides were purified by reverse-phase high-performance liquid chromatography using a gradient of water of acetonitrile with 0.1% TFA; excess residual TFA was removed by chromatography on a Stratosphere SPE column (Varian) using 0.1% formic acid as the ion-pairing agent. Stock peptide concentrations were determined using ^{19}F NMR with a known concentration of TFA as a reference. Peptide identities were confirmed using matrix-assisted laser desorption ionization mass spectroscopy.

Lipid Preparation. 1,2-Dimyristoyl-*sn*-glycero-3-phosphocholine (DMPC), 1,2-dimyristoyl-*sn*-glycero-3-phospho(1′-*rac*-glycerol) (DMPG), 1,2-dihexanoyl-*sn*-glycero-3-phosphocholine (DHPC), and dodecylphosphocholine (DPC) were purchased from Affymetrix. Isotropic bicelles were created in PBS buffer (pH 7.4) with 10% D_2O by adding a 3:1 DMPC/DMPG solution to a solution of DHPC giving a q of 0.5 resulting in a clear, nonviscous solution.

Determinations of MICs. The peptide minimum inhibitory concentrations (MICs) against *Escherichia coli* K12 were determined

by the microdilution antimicrobial assay procedure, using 96-well plates in replicates of four, as described previously.[41]

^{1}H NMR. Samples were prepared in PBS (pH 6.0) containing 10% D_2O, 100 mM DPC, and 400 μM peptide. Spectra were recorded at 30 °C using a Varian VNMRS 500 MHz NMR spectrometer. A water suppression pulse sequence (WET) was employed in the acquisition of NMR spectra.

^{19}F NMR. All ^{19}F NMR experiments were performed at 30 °C using a Varian VNMRS 500 MHz NMR spectrometer equipped with a double-tuned ^{1}H−^{19}F room-temperature probehead. Peptide and lipid samples were prepared with 10% D_2O in PBS (pH 7.4). All experiments were performed at a constant peptide concentration of 400 μM unless indicated otherwise and referenced to an external standard of trifluoroacetate ion (at 0 ppm) in PBS (pH 7.4) and 10% D_2O. To measure solvent isotope-induced changes in chemical shifts, peptide and lipid samples were first prepared with 10% D_2O in PBS (pH 7.4). The samples were then lyophilized overnight and redissolved in 90% D_2O.

^{19}F CPMG relaxation dispersion experiments were performed for the peptides in the free state and in the presence of lipid bicelles (total lipid concentration of 200 mM; q = 0.5; long chain lipids in a 3:1 DMPC:DMPG molar ratio and the short chain lipid being DHPC). CPMG delays (τ_{cp}) were varied from 0.5 to 10.0 ms with each data point recorded as a series of standard one-dimensional transverse relaxation rate measurements with T_2 delays of 0.05, 0.1, 0.2, 0.4, 0.8, and 1.6 ms for the free peptide and 0.0125, 0.025, 0.05, 0.1, 0.2, and 0.4 ms for the bicelle-bound peptide. The pulse width was 7.9 μs. Data sets were recorded with an acquisition time of 1 s in T_1 along with a 10 s prescan delay. Sixteen scans, with a net acquisition time of 17 min/data point, were required to achieve adequate signal-to-noise ratios for peptides in the free state; 32 scans, with a net acquisition time of 35 min/data point, were required to achieve adequate signal-to-noise ratios for peptides bound to bicelles. ^{19}F spin−lattice relaxation times (T_1) were acquired by an inversion recovery sequence (180°−τ−90°) using a total of six τ values of 0.0625, 0.125, 0.25, 0.5, 1.0, and 2.0 s. Data were processed and analyzed using VNMRJ and plotted using Kaleidagraph.

All other experimental details have been described previously.[37,42]

RESULTS

We previously demonstrated the feasibility of using fluorine-labeled amino acids to probe the chemical environment and dynamics of membrane-bound peptides containing TfeG.[37] TfeG provides a useful probe, as it is relatively small (approximately comparable to valine), is commercially available, and is readily incorporated into peptides. The C-3 methylene group affords one degree of rotational motion to the trifluoromethyl group, but on the time scale of our experiments, backbone dynamics are likely to dominate its NMR behavior. Although substitution of hydrophilic residues, such as lysine, with TfeG obviously cannot be considered as conservative, numerous experiments with AMPs have shown that their biological properties and structure depend primarily on their overall physicochemical properties and are not highly dependent on sequence. Changes to a single site usually minimally perturb structure and activity.

In studies of two MSI-78 variants[37] incorporating TfeG at a positively charged exterior position (Lys-7) and a hydrophobic position (Leu-6), we demonstrated position-dependent changes in ^{19}F chemical shifts and transverse relaxation times upon peptide binding to small unilamellar vesicles and lipid bicelles.

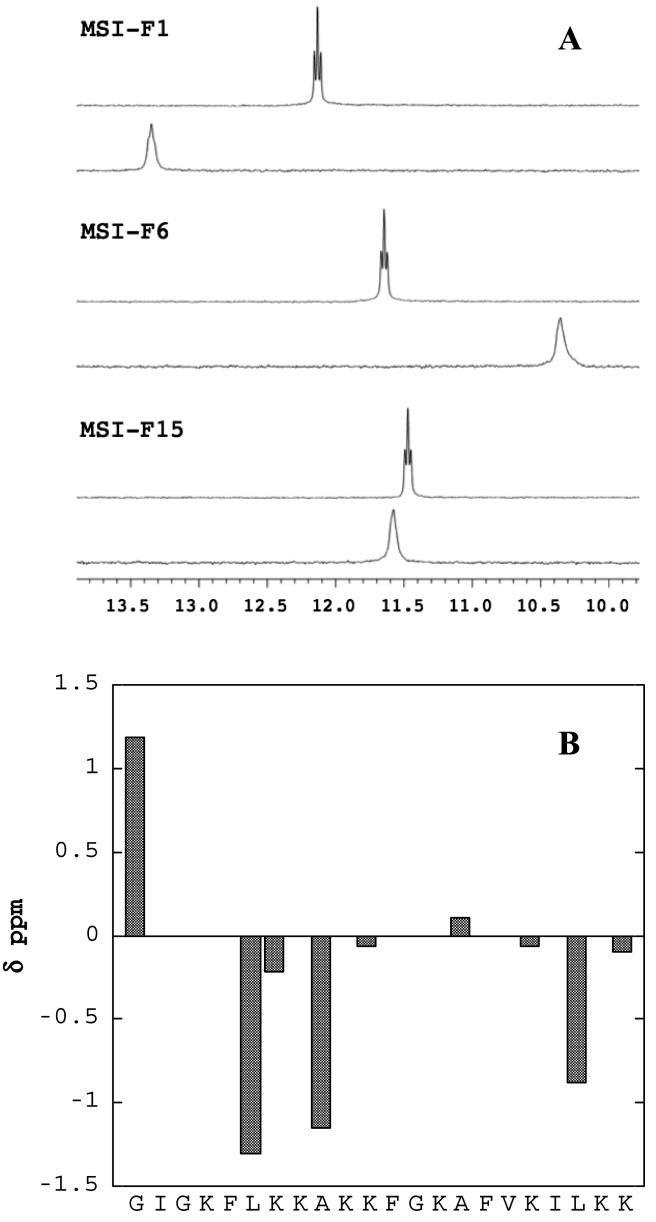

Figure 3. (A) Representative ^{19}F NMR spectra illustrating changes in chemical shift and peak width that occur when TfeG-substituted peptides bind to lipid bicelles. The top trace in each pair of spectra is of the free peptide and the bottom trace the peptide bound to the bicelles. Spectra were recorded at 30 °C and pH 7.4 in PBS buffer with 10% D_2O and referenced to an external TFA standard at 0 ppm. (B) Chemical shift changes, $\Delta\delta$, associated with peptide binding to bicelles plotted as a function of label position.

Whereas these initial studies provided a "proof of concept", we considered it important to conduct a more comprehensive study to determine, more generally, how sensitive fluorine probes are for distinguishing chemical environment and local dynamics.

In this work, we have extended our investigation by synthesizing a series of nine MSI-78 variants in which TfeG has been introduced at strategic positions throughout the 22-residue peptide. (We name these peptides as MSI-Fn,[a] when n refers to the position in the peptide that has been substituted with the fluorinated amino acid.) Guided by the NMR structure of the peptide bound to lipids,[31] we introduced TfeG at four hydrophobic

Table 1. ^{19}F Chemical Shifts and R_1 and R_2 Values for MSI-F Peptides

peptide	amino acid substituted	δ_{free}[a] (ppm)	δ_{bound}[a] (ppm)	R_{1free} (Hz)	R_{1bound} (Hz)	R_{2free}[b] (Hz)	R_{2bound}[b] (Hz)
MSI-F1	Gly	12.15	13.34	1.40 ± 0.05	2.55 ± 0.06	1.7 ± 0.1	27 ± 1
MSI-F6	Leu	11.64	10.34	2.18 ± 0.05	3.09 ± 0.04	3.7 ± 0.2	58 ± 9
MSI-F7	Lys	11.64	11.42	2.31 ± 0.03	3.10 ± 0.14	3.7 ± 0.2	22 ± 2
MSI-F9	Ala	11.73	10.58	2.37 ± 0.05	3.10 ± 0.14	4.1 ± 0.2	43 ± 3
MSI-F11	Lys	11.55	11.49	2.30 ± 0.04	3.06 ± 0.05	4.1 ± 0.2	27 ± 3
MSI-F15	Ala	11.47	11.58	2.26 ± 0.05	3.86 ± 0.11	3.9 ± 0.1	49 ± 3
MSI-F18	Lys	11.51	11.45	2.23 ± 0.05	3.24 ± 0.07	3.1 ± 0.1	29 ± 2
MSI-F20	Leu	11.60	10.72	2.05 ± 0.03	3.12 ± 0.09	2.8 ± 0.2	36 ± 2
MSI-F22	Lys	11.40	11.30	1.53 ± 0.06	2.27 ± 0.05	2.1 ± 0.2	20 ± 0.4
TfeG		11.62		0.54 ± 0.03		1.1 ± 0.1	

[a] Chemical shift relative to external TFA. [b] Value when $1/\tau_{cp}$ = 2000 Hz.

positions and at four lysine residues spaced along the length of the peptide, including the C-terminal residue Lys-22; we also substituted the N-terminal glycine, which may be expected to show a large change in mobility. The positions that were substituted are shown in Figure 2. For each peptide, we have measured the changes in ^{19}F chemical shifts, longitudinal and transverse relaxation rates (R_1 and R_2, respectively), and D_2O-induced ^{19}F chemical shifts that occur upon peptide binding to lipid bicelles. This has allowed us to obtain a detailed picture of the local changes in chemical environment peptide dynamics that occur when MSI-78 binds to the lipid bilayer.

Effects of TfeG Substitution on Secondary Structure and Biological Activity. Substitution of TfeG at different positions in these peptides does not appear to cause any gross structural changes or changes in biological activity. The MIC values for all the peptides were within the range of 3−6 μg/mL against *E. coli* K12 strains; any differences in MICs between the parent MSI-78 peptide[32] and the TfeG-labeled peptides were not statistically significant. The peptides all appear to adopt a predominantly random coil structure in plain buffer and exhibit extensively helical CD spectra in the presence of SDS micelles (see the Supporting Information). The mean residue ellipticities, Θ_{222}, of the peptides varied by less than 10% (-20200 cm^2 dmol^{-1} residue^{-1} > Θ_{222} > -21900 cm^2 dmol^{-1} residue^{-1}) between the different peptides and are similar to that of MSI-78 (Θ_{222} = -20700 cm^2 dmol^{-1} residue^{-1}).

As a further check on the structural integrity of the TfeG-labeled peptides, one-dimensional proton NMR spectra of the peptides were recorded for the peptides bound to DPC micelles (see the Supporting Information). In each case, the peptides exhibited well-dispersed resonances in the amide region, characteristic of structured peptides. As expected, small changes between the spectra of each TfeG-labeled peptide and MSI-78 were observed, which may reflect small local structural changes and/or slight differences in sample preparation. The resonances from the three Phe side chains in the peptide could clearly be distinguished and were very similar in each case, indicating that the hydrophobic core of the dimeric peptide bundle remains intact. Resonances from the aliphatic side chains were obscured by signals from the lipid bicelles.

Sensitivity of ^{19}F Chemical Shifts to the Position of Fluorination. In the absence of lipids, all the peptides, except MSI-F1, exhibited a sharp triplet in the ^{19}F NMR spectrum between 11.40 and 11.73 ppm relative to TFA (Figure 3 and Table 1). The resonance for MSI-F1, in which Gly is substituted with TfeG, is shifted significantly downfield at 12.15 ppm. This is likely due to the influence of the positively charged amino group at the N-terminus.

We then examined the binding of the fluorinated MSI-78 variants to lipid bicelles, which are commonly used as a model membrane system. (As we have discussed previously,[37] for these studies bicelles are preferable to SUVs, which are also commonly used to study AMP−membrane interactions. Bicelles are more stable than SUVs and present a flat, rather than highly curved, surface for peptide binding.) All the peptides exhibited distinct changes in their ^{19}F chemical shifts upon binding to bicelles, which appeared as broadened single peaks (Figure 3).

The change in chemical shift was highly dependent on the position of the TfeG residue (Table 1), demonstrating the sensitivity of the ^{19}F nucleus to the local chemical environment. The positions that exhibited the largest upfield shifts, ranging from −0.9 to −1.3 ppm, are those at hydrophobic positions that are deeply buried in the core of the coiled coil (Figure 4). The lysine positions, which project out from the coiled coil and interact with the lipid headgroups, exhibited smaller upfield shifts ranging from −0.06 to −0.26 ppm. Two positions seem to deviate from this general trend. Substituting TfeG at the N-terminal glycine position (MSI-F1) results in a large downfield shift of 1.2 ppm; MSI-F15, in which Ala is substituted by TfeG, also showed a downfield shift, although this was quite small, only 0.09 ppm.

Although fluorine chemical shifts are influenced by various factors,[43] the "anomalous" chemical shift of MSI-F15 might be explained by the fact that the TfeG side chain is expected to protrude toward the charged face of the α-helix (Figure 4). Its chemical shift is likely to be influenced by the positively charged lysine residues that are adjacent to it; this could result in deshielding of the nucleus and thereby shift the resonance to lower field. In contrast, substitution of Ala-9 with TfeG (MSI-F9) places the side chain pointing into the hydrophobic core (Figure 4), presumably resulting in a more shielded environment. The downfield shift observed when TfeG is at the N-terminal position is harder to explain. Possibly, in its folded state, the N-terminus of the peptide is less well solvated so that the deshielding effect of the positively charged amino terminus is greater. The N-terminus is also in the proximity of the amino group of the C-terminal lysine of the peptide forming the opposite strand of the coiled coil, which could also influence the fluorine chemical shift.

Changes in Solvent Exposure upon Binding to Lipid Bicelles. The ^{19}F chemical shift is sensitive to the isotopic composition of the solvent, e.g., whether H_2O or D_2O,[16,18] and this provides a means to investigate changes in solvent exposure that may occur when MSI-78 binds to lipid bilayers. In the absence of bicelles, changing the solvent composition from

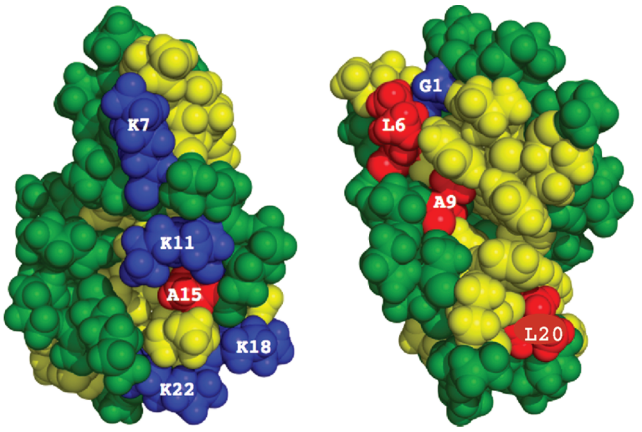

Figure 4. Space filling models of the MSI-78 dimer illustrating the chemical environment of the positions substituted with TfeG. Residues substituted with TfeG are colored blue (hydrophilic) and red (hydrophobic). Other hydrophobic and hydrophilic residues are colored yellow and green, respectively. For the sake of clarity, the substituted positions are shown on only one peptide of the dimer. The two structures are related to each other by an ~180° rotation about the vertical axis.

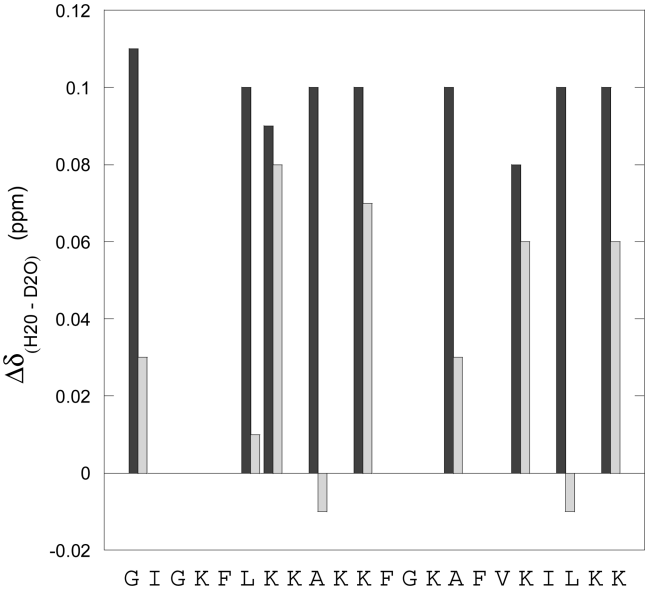

Figure 5. Effects of solvent isotopes on ^{19}F chemicals shift ($\Delta\delta_{H_2O-D_2O}$) plotted as a function of label position. Dark gray bars show data for peptides free in solution; light gray bars show data for peptides bound to lipid bicelles.

10% D_2O to 90% D_2O results in the ^{19}F chemical shift for each of the peptides moving fairly uniformly upfield by 0.08−0.11 ppm (see Figure 5). In the presence of bicelles, the chemical shift changes, $\Delta\delta_{H_2O-D_2O}$ ($\Delta\delta_{H_2O-D_2O} = \delta_{H_2O} - \delta_{D_2O}$), are more variable and range from −0.01 to 0.08 ppm (changes of ≤0.01 ppm were not considered significant). In theory, positions that are deeply buried should exhibit no changes in chemical shift with a change in the solvent, whereas positions that are completely exposed should exhibit changes similar to those observed for the unbound peptides. Inspection of the data reveals this to be qualitatively true: positions 7, 11, 18, and 22, which are occupied

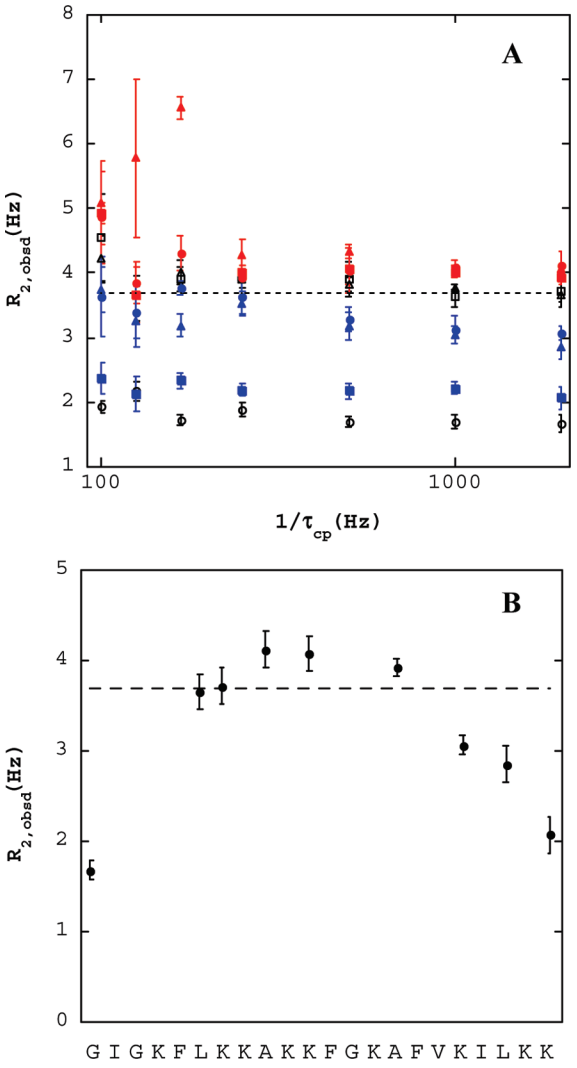

Figure 6. (A) Observed transverse relaxation rates, $R_{2,observed}$, for MSI-F peptides in free solution plotted as a function of CPMG pulsing rate ($1/\tau_{cp}$): MSI-F1 (○), MSI-F6 (△), MSI-F7 (□), MSI-F9 (red filled circles), MSI-F11 (red filled triangles), MSI-F15 (red filled squares), MSI-F18 (●), MSI-F20 (▲), and MSI-F22 (■). (B) Transverse relaxation rates for peptides plotted as a function of sequence. The data were obtained using a $1/\tau_{cp}$ values of 2000 Hz, so that the chemical exchange component is removed. The calculated R_2 of 3.7 Hz for free peptide is indicated by the dashed line.

by lysines in MSI-78, exhibit the largest chemical shift changes ($\Delta\delta_{H_2O-D_2O}$ = 0.08−0.06 ppm). These are somewhat smaller than those observed for the free peptide, indicating that interactions with the lipid headgroups may reduce the level of solvent exposure. In contrast, at positions 6, 9, 15, and 20, which are occupied by hydrophobic residues in MSI-78, $\Delta\delta_{H_2O-D_2O}$ is very small (−0.01 to 0.03 ppm). This indicates a very low degree of solvent exposure in the bound state and provides support for the proposed structural model of MSI-78 in which these positions form part of the hydrophobic core of the coiled coil peptide dimer in the membrane.

Various studies of fluorinated proteins have shown that ^{19}F longitudinal relaxation rates ($R_1 = 1/T_1$) are generally faster for buried residues in proteins than for solvent-exposed residues,[16,18] and these measurements have been used to probe protein

structure and folding. Therefore, we also investigated how R_1 changed when the peptides bound to bicelles. The R_1 values for the free peptides range from 1.4 to 2.4 Hz, with the terminal residues exhibiting the lowest R_1 values (Table 1). The R_1 values increase fairly uniformly for the peptides on binding bicelles with R_1 values ranging from 2.3 to 3.9 Hz (Table 1). It appears that longitudinal relaxation measurements are not especially sensitive to differences in the local chemical environment for this particular system.

Changes in Peptide Dynamics Probed by ^{19}F Transverse Relaxation Rates. The transverse relaxation rates of the free peptides (R_{2f}) were measured using a CPMG experiment in which $1/\tau_{cp}$ was varied from 100 to 2000 Hz. For all the peptides, R_2 values are similar and are independent of τ_{cp} (Figure 5A), as expected for an unstructured peptide in free solution. The experimental R_2 values (Figure 5B) generally agree well with that calculated for a random coil peptide in free solution;[37] however, residues at the N- and C-termini exhibit significantly slower R_{2f} values (Figure 5B and Table 1). This indicates that the ends of the peptide are more mobile than the center, which would be expected for an unstructured peptide chain.

The transverse relaxation rates were measured for each peptide bound to bicelles, R_{2b}, using the same set of CPMG pulse sequences. Under the conditions used in the experiment, nearly all of the peptide was bound to the lipid bilayer (as shown in Figure 3, no signal for the free peptide could be detected). As discussed previously,[37,44,45] when τ_{cp} is short relative to the residence time, τ_b, of the peptide in the lipid, the observed R_{2b} values reflect the intrinsic relaxation rates of the ^{19}F nuclei unencumbered by chemical exchange. Under these conditions, differences in R_{2b} may be attributed to changes in the local dynamics of the peptide.

The observed R_{2b} values for all the peptides were essentially invariant for values of $1/\tau_{cp}$ greater than 250 Hz, consistent with our previous results.[37] At longer pulse intervals, R_{2b} appears to increase, indicative of chemical exchange (Figure 6A). However, at these time scales, the experiment approaches the limits of sensitivity because of interconversion between in-phase and antiphase magnetization during the spin−echo period, as well as loss of signal intensity due to chemical exchange. Therefore, measurements are accompanied by large uncertainty in the value of R_{2b}, and τ_b cannot be reliably determined from the data. However, the experiment does allow us to put an upper limit on the rate at which the peptide dissociates from the membrane ($1/\tau_b$) of ~200 s^{-1}, consistent with our previous data.

The transverse relaxation rates measured for the CF_3 reporter group varied significantly depending upon the location of the reporter nuclei (Figure 6B). The R_{2b} values for each of the peptides determined at a $1/\tau_{cp}$ of 2000 Hz are listed in Table 1. The hydrophobic positions exhibit the fastest relaxation rates (e.g., Leu-6, R_{2b} = 58 Hz; Ala-15, R_{2b} = 49 Hz), indicating that these residues, which are predicted to be in the hydrophobic core of the coiled coil, are relatively immobile. Moreover, the relaxation rates are close to the theoretical value, ~50 Hz, predicted if relaxation is dominated by the tumbling motion of the lipid bicelle.

Hydrophilic positions, which are predicted to be on the surface of the coiled coil and interact with lipid headgroups, exhibit slower relaxation rates, indicating that these positions have greater mobility. The R_{2b} values do not vary greatly along the length of the peptide [e.g., Gly-1 (28 Hz), Lys-11 (27 Hz), and Lys-18 (29 Hz)], although the C-terminal lysine appears to be slightly more mobile. These data suggest that the N-terminus is

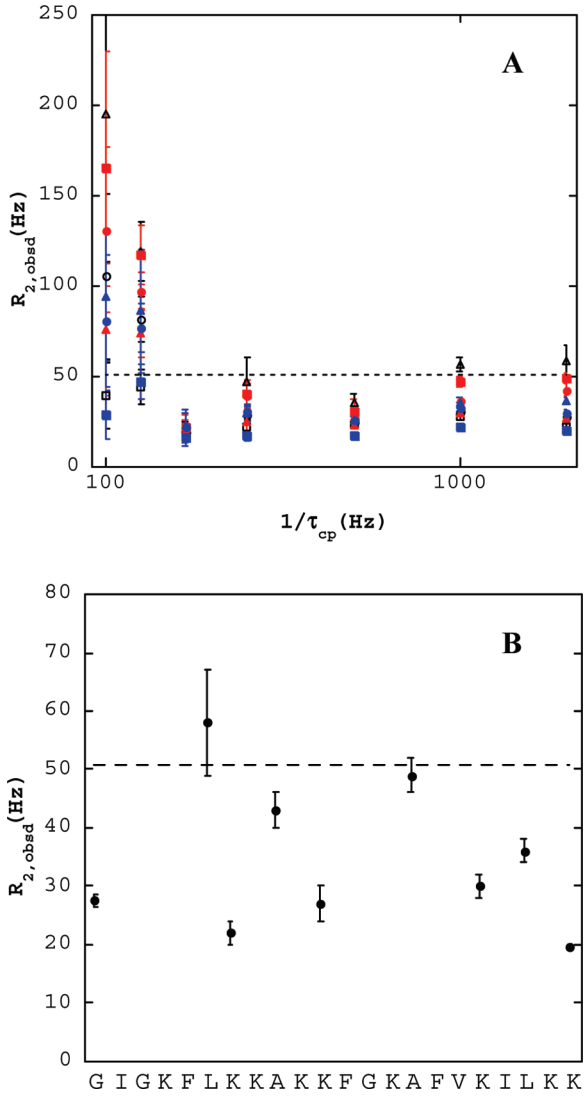

Figure 7. (A) Observed transverse relaxation rates, $R_{2,observed}$, for MSI-F peptides bound to lipid bicelles plotted as a function of CPMG pulsing rate ($1/\tau_{cp}$): MSI-F1 (○), MSI-F6 (△), MSI-F7 (□), MSI-F9 (red filled circles), MSI-F11 (red filled triangles), MSI-F15 (red filled squares), MSI-F18 (●), MSI-F20 (▲), and MSI-F22 (■). (B) Transverse relaxation rates for peptides plotted as a function of the position of the TfeG probe within the peptide sequence. The data were obtained using a $1/\tau_{cp}$ of 2000 Hz, so that the chemical exchange component is removed. The calculated R_2 of 50.8 Hz for the peptide bound to lipid bicelles (assuming relaxation is only due to tumbling of bicelles) is indicated by the dashed line.

quite well structured when bound to the lipid and does not appear to undergo fraying on the time scale of these experiments. This is consistent with the significant degree of solvent protection observed for the N-terminus in the solvent isotope effect study. The C-terminus of the peptide is more dynamic, but compared to that of the free peptide, it is clearly less mobile and better structured.

The changes in chemical shifts and transverse relaxation rates observed when the peptides bind to bicelles appear to be independent of each other. Thus, although the positions occupied by Ala-9 and Ala-15 both appear to be quite immobile (R_{2b} = 43 and 49 Hz, respectively), Ala-9 shifts downfield by 1.15 ppm whereas Ala-15

shifts slightly upfield by −0.11 ppm. The chemical shifts of N- and C-terminal positions change in opposite directions (1.19 and −0.10 ppm, respectively) even though both positions exhibit similar mobilities as judged by their R_{2b} values (Figure 7).

DISCUSSION

Solution-phase ^{19}F NMR has been used to study the dynamics of integral membrane proteins and the interactions of other proteins with membranes;[46−49] these studies use proteins labeled with fluorinated tryptophan, phenylalanine, and tyrosine analogues that can readily be incorporated biosynthetically. Our studies extend the use of ^{19}F NMR to examine the more transient and dynamic interactions of peptides with membranes and provide position-specific information about how the chemical environment and dynamics of residues in MSI-78 change upon binding to the lipid bilayer. The results show that ^{19}F NMR is a sensitive and generally useful method for interrogating peptide−membrane interactions in free solution.

Changes in ^{19}F chemical shift provide a simple way of detecting binding at concentrations that are close to those at which the peptide is biologically active. For MSI-78, spectral shifts were apparent for all the TfeG-labeled peptides, regardless of the position of the label. In these studies, spectra were recorded on a 500 MHz spectrometer at a peptide concentration of 400 μM to facilitate CPMG experiments; however, 40 μM TfeG-labeled peptide is readily detected at a signal-to-noise ratio of 4:1 after 64 scans in a spectrum that takes only 2 min to acquire. Another advantage is that the wide range of chemical shift changes observed potentially allows multiple peptides to be studied in one experiment (or multiple fluorine probes to be introduced into one peptide), so that more complex multicomponent interactions can be studied.

Effects of solvent isotopes (H_2O vs D_2O) on the fluorine chemical shift have been employed to study the structure and dynamics of large proteins.[16,18] Our results demonstrate that this technique also provides a simple but effective probe of peptide−membrane interactions. In this case, it is evident that, even when embedded in the membrane, the lysine positions remain predominantly solvated whereas the hydrophobic positions are extensively shielded from the solvent. This supports the model in which MSI-78 forms toroidal pores in the lipid bilayer,[30] in which the lysine side chains interact with hydrophilic lipid headgroups.

From the measurements of transverse relaxation rates along the peptide backbone, we have obtained detailed information about the local dynamics of MSI-78 bound to the lipid bilayer. The hydrophobic positions of the amphipathic peptide that form the core of the coiled coil are the least dynamic positions. This suggests a well-packed core in which side chain rotations are restricted. The positively charged face of the coiled coil, which interacts with the hydrophilic lipid headgroups, is more dynamic, although far less so than in the unbound peptide. Moreover, positions toward the center of the peptide appear to be less dynamic than the ends of the peptide. This would be consistent with the peptides forming toroidal pores in the lipid bilayer, as has been deduced for MSI-78. If we assume the peptide sits centrally in the pore, the constriction of the peptide by the lipid bilayer would by greatest at the center of the pore, where the opening is narrowest.

The ^{19}F transverse relaxation data provide new and more detailed information about the local dynamics of peptide upon binding to a lipid membrane. The changes in ^{19}F chemical shifts can only be interpreted qualitatively using the structural model of MSI-78 determined by NMR.[31] However, density functional theory methods have been used to calculate ^{19}F chemical shifts for a large number of fluorinated small molecules[50,51] with a reasonable degree of accuracy. In a study particularly pertinent to our experiments, it was found that hindered rotation of CF_3 groups led to an upfield shift of the ^{19}F signal.[51] Future advances in computational methods will likely allow ^{19}F chemical shifts in fluorinated peptides and proteins to be calculated. This would permit the relationship among structure, dynamics, and chemical shift to be quantitatively understood, providing a further tool for analyzing peptide−membrane interactions.

In conclusion, these studies demonstrate that ^{19}F NMR provides a relatively sensitive and general technique for investigating the interactions of peptides and proteins with their membrane targets. In particular, the chemical shift and transverse relaxation rates are highly sensitive to the position of the fluorine label in the peptide and provide information about changes in local peptide motions. Future work will aim toward using fluorine NMR to study peptide−membrane interactions in vivo at physiologically relevant concentrations.

ASSOCIATED CONTENT

Supporting Information. Circular dichroism spectra, proton NMR spectra, and tables of MICs and of $R_{2observed}$ values determined in CMPG experiments. This material is available free of charge via the Internet at http://pubs.acs.org.

AUTHOR INFORMATION

Corresponding Author

*Department of Chemistry, University of Michigan, Ann Arbor, MI 48109-1055. E-mail: nmarsh@umich.edu. Phone: (734) 763-6096. Fax: (734) 615-3790.

Notes

[a]In our initial publication, we referred to two TfeG-containing peptides as MSI-F1 and MSI-F2, where the numeric designation did not imply any positional information. Because we have adopted a more systematic nomenclature in this study, these peptides must be relabeled so that MSI-F1 is now MSI-F7 and MSI-F2 is now MSI-F6. We apologize to the reader for the confusion this may cause.

Funding Sources

This research was supported by National Science Foundation Grant CHE 0640934 to E.N.G.M.

ACKNOWLEDGMENT

We thank Dr. Jeetender Chugh for helpful discussions and advice on CPMG experiments.

ABBREVIATIONS

AMP, antimicrobial peptide; TfeG, L-4,4,4,-trifluoroethylglycine; MIC, minimum inhibitory concentrations; DMPC, 1,2-dimyristoyl-*sn*-glycero-3-phosphocholine; DMPG, 1,2-dimyristoyl-*sn*-glycero-3-phospho(1′-*rac*-glycerol); DHPC, 1,2-dihexanoyl-*sn*-glycero-3-phosphocholine; CPMG, Carr−Purcell−Meiboom−Gill.

REFERENCES

(1) Brogden, K. A. (2005) Antimicrobial peptides: Pore formers or metabolic inhibitors in bacteria?. *Nat. Rev. Microbiol.* 3, 238–250.

(2) Dennison, S. R., Whittaker, M., Harris, F., and Phoenix, D. A. (2006) Anticancer α-helical peptides and structure/function relationships underpinning their interactions with tumour cell membranes. *Curr. Protein Pept. Sci. 7*, 487–499.

(3) Dhople, V., Krukemeyer, A., and Ramamoorthy, A. (2006) The human β-defensin-3, an antibacterial peptide with multiple biological functions. *Biochim. Biophys. Acta 1758*, 1499–1512.

(4) Gennaro, R., and Zanetti, M. (2000) Structural features and biological activities of the cathelicidin-derived antimicrobial peptides. *Biopolymers 55*, 31–49.

(5) Koyama, Y., Motobu, M., Hikosaka, K., Yamada, M., Nakamura, K., Saido-Sakanaka, H., Asaoka, A., Yamakawa, M., Sekikawa, K., Kitani, H., Shimura, K., Nakai, Y., and Hirota, Y. (2006) Protective effects of antimicrobial peptides derived from the beetle *Allomyrina dichotoma* defensin on endotoxic shock in mice. *Int. Immunopharmacol. 6*, 234–240.

(6) Nomura, K., and Corzo, G. (2006) The effect of binding of spider-derived antimicrobial peptides, oxyopinins, on lipid membranes. *Biochim. Biophys. Acta 1758*, 1475–1482.

(7) Ramamoorthy, A., Thennarasu, S., Lee, D. K., Tan, A. M., and Maloy, L. (2006) Solid-state NMR investigation of the membrane-disrupting mechanism of antimicrobial peptides MSI-78 and MSI-594 derived from magainin 2 and melittin. *Biophys. J. 91*, 206–216.

(8) Porcelli, F., Verardi, R., Shi, L., Henzler-Wildman, K. A., Ramamoorthy, A., and Veglia, G. (2008) NMR structure of the cathelicidin-derived human antimicrobial peptide LL-37 in dodecylphosphocholine micelles. *Biochemistry 47*, 5565–5572.

(9) Powers, J. P. S., Tan, A., Ramamoorthy, A., and Hancock, R. E. W. (2005) Solution structure and interaction of the antimicrobial polyphemusins with lipid membranes. *Biochemistry 44*, 15504–15513.

(10) Porcelli, F., Buck, B., Lee, D. K., Hallock, K. J., Ramamoorthy, A., and Veglia, G. (2004) Structure and orientation of pardaxin determined by NMR experiments in model membranes. *J. Biol. Chem. 279*, 45815–45823.

(11) Mani, R., Cady, S. D., Tang, M., Waring, A. J., Lehrer, R. I., and Hong, M. (2006) Membrane-dependent oligomeric structure and pore formation of β-hairpin antimicrobial peptide in lipid bilayers from solid-state NMR. *Proc. Natl. Acad. Sci. U.S.A. 103*, 16242–16247.

(12) Wu, X., Mani, R., Tang, M., Buffy, J. J., Waring, A. J., Sherman, M. A., and Hong, M. (2006) Membrane-Bound Dimer Structure of a β-Hairpin Antimicrobial Peptide from Rotational-Echo Double-Resonance Solid-State NMR. *Biochemistry 45*, 8341–8349.

(13) Afonin, S., Grage, S. L., Ieronimo, M., Wadhwani, P., and Ulrich, A. S. (2008) Temperature-Dependent Transmembrane Insertion of the Amphiphilic Peptide PGLa in Lipid Bilayers; Observed by Solid State F-19 NMR Spectroscopy. *J. Am. Chem. Soc. 130*, 16512–16513.

(14) Buffy, J. J., Waring, A. J., and Hong, M. (2005) Determination of peptide oligomerization in lipid bilayers using F-19 spin diffusion NMR. *J. Am. Chem. Soc. 127*, 4477–4483.

(15) Ieronimo, M., Afonin, S., Koch, K., Berditsch, M., Wadhwani, P., and Ulrich, A. S. (2010) F-19 NMR Analysis of the antimicrobial peptide PGLa bound to native cell membranes from bacterial protoplasts and human erythrocytes. *J. Am. Chem. Soc. 132*, 8822–8823.

(16) Evanics, F., Bezsonova, I., Marsh, J., Kitevski, J. L., Forman-Kay, J. D., and Prosser, R. S. (2006) Tryptophan solvent exposure in folded and unfolded states of an SH3 domain by F-19 and H-1 NMR. *Biochemistry 45*, 14120–14128.

(17) Hull, W. E., and Sykes, B. D. (1974) Fluorotyrosine alkaline phosphatase: ^{19}F NMR relaxation times and molecular motion of individual fluorotyrosines. *Biochemistry 13*, 3431–3437.

(18) Hull, W. E., and Sykes, B. D. (1976) Fluorine-19 NMR study of fluorotyrosine alkaline phosphatase: Influence of zinc on protein structure and conformational change induced by phosphate binding. *Biochemistry 15*, 1535–1546.

(19) Kitevski-LeBlanc, J. L., Evanics, F., and Prosser, R. S. (2009) Approaches for the measurement of solvent exposure in proteins by F-19 NMR. *J. Biomol. NMR 45*, 255–264.

(20) Prosser, R. S., Luchette, P. A., Westerman, P. W., Rozek, A., and Hancock, R. E. W. (2001) Determination of membrane immersion depth with O-2: A high-pressure F-19 NMR study. *Biophys. J. 80*, 1406–1416.

(21) Huang, H. W., Chen, F.-Y., and Lee, M.-T. (2004) Molecular mechanism of peptide-induced pores in membranes. *Phys. Rev. Lett. 92*, 19304–19310.

(22) Oren, Z., and Shai, Y. (1998) Mode of action of linear amphipathic α-helical antimicrobial peptides. *Biopolymers 47*, 451–463.

(23) Wimley, W. C. (2010) Describing the mechanism of antimicrobial peptide action with the interfacial activity model. *ACS Chem. Biol. 5*, 905–917.

(24) Hancock, R. E. W., and Lehrer, R. (1998) Cationic peptides: A new source of antibiotics. *Trends Biotechnol. 16*, 82–88.

(25) Shai, Y. (1999) Mechanism of the binding, insertion and destabilization of phospholipid bilayer membranes by α-helical antimicrobial and cell non-selective membrane-lytic peptides. *Biochim. Biophys. Acta 1462*, 55–70.

(26) Wu, M. H., Maier, E., Benz, R., and Hancock, R. E. W. (1999) Mechanism of interaction of different classes of cationic antimicrobial peptides with planar bilayers and with the cytoplasmic membrane of *Escherichia coli*. *Biochemistry 38*, 7235–7242.

(27) Epand, R. F., Ramamoorthy, A., and Epand, R. M. (2006) Membrane lipid composition and the interaction with Pardaxin: The role of cholesterol. *Protein Pept. Lett. 13*, 1–5.

(28) Oren, Z., and Shai, Y. (1997) Selective lysis of bacteria but not mammalian cells by diastereomers of melittin: Structure-function study. *Biochemistry 36*, 1826–1835.

(29) Selsted, M. E., Novotny, M. J., Morris, W. L., Tang, Y. Q., Smith, W., and Cullor, J. S. (1992) Indolicidin, a novel bactericidal tridecapeptide amide from neutrophils. *J. Biol. Chem. 267*, 4292–4295.

(30) Hallock, K. J., Lee, D. K., and Ramamoorthy, A. (2003) MSI-78, an analogue of the magainin antimicrobial peptides, disrupts lipid bilayer structure via positive curvature strain. *Biophys. J. 84*, 3052–3060.

(31) Porcelli, F., Buck-Koehntop, B. A., Thennarasu, S., Ramamoorthy, A., and Veglia, G. (2006) Structures of the dimeric and monomeric variants of magainin antimicrobial peptides (MSI-78 and MSI-594) in micelles and bilayers, determined by NMR spectroscopy. *Biochemistry 45*, 5793–5799.

(32) Gottler, L. M., Lee, H. Y., Shelburne, C. E., Ramamoorthy, A., and Marsh, E. N. G. (2008) Using fluorous amino acids to modulate the biological activity of an antimicrobial peptide. *ChemBioChem 9*, 370–373.

(33) Gottler, L. M., De la Salud-Bea, R., Shelburne, C. E., Ramamoorthy, A., and Marsh, E. N. G. (2008) Using fluorous amino acids to probe the effects of changing hydrophobicity on the physical and biological properties of the β-hairpin antimicrobial peptide protegrin-1. *Biochemistry 47*, 9243–9250.

(34) Hsieh, K. H., Needleman, P., and Marshall, G. R. (1987) Long-acting angiotensin-II inhibitors containing hexafluorovaline in position-8. *J. Med. Chem. 30*, 1097–1100.

(35) Wang, P., Tang, Y., and Tirrell, D. A. (2003) Incorporation of trifluoroisoleucine into proteins in vivo. *J. Am. Chem. Soc. 125*, 6900–6906.

(36) Meng, H., and Kumar, K. (2007) Antimicrobial activity and protease stability of peptides containing fluorinated amino acids. *J. Am. Chem. Soc. 129*, 15615–15622.

(37) Buer, B. C., Chugh, J., Al-Hashimi, H. M., and Marsh, E. N. G. (2010) Using fluorine NMR to probe the interaction of membrane-active peptides with the lipid bilayer. *Biochemistry 49*, 5760–5765.

(38) Tsushima, T., Kawada, K., Ishihara, S., Uchida, N., Shiratori, O., Higaki, J., and Hirata, M. (1988) Fluorine-containing amino-acids and their derivatives. 7. Synthesis and antitumor-activity of α-substituted and γ-substituted methotrexate analogs. *Tetrahedron 44*, 5375–5387.

(39) Lee, H. Y., Lee, K. H., Al-Hashimi, H. M., and Marsh, E. N. G. (2006) Modulating protein structure with fluorous amino acids: Increased stability and native-like structure conferred on a 4-helix bundle protein by hexafluoroleucine. *J. Am. Chem. Soc. 128*, 337–343.

(40) Gottler, L. M., de la Salud-Bea, R., and Marsh, E. N. G. (2008) The fluorous effect in proteins: Properties of α4F6, a 4-α-helix bundle protein with a fluorocarbon core. *Biochemistry 47*, 4484–4490.

(41) Shelburne, C. E., An, F. Y., Dholpe, V., Ramamoorthy, A., Lopatin, D. E., and Lantz, M. S. (2007) The spectrum of antimicrobial activity of the bacteriocin subtilosin A. *J. Antimicrob. Chemother. 59*, 297–300.

(42) Huhta, M. S., Chen, H.-P., Hemann, C., Hille, C. R., and Marsh, E. N. G. (2001) Protein-coenzyme interactions in adenosylcobalamin-dependent glutamate mutase. *Biochem. J. 355*, 131–137.

(43) Lau, E. Y., and Gerig, J. T. (2000) Origins of fluorine NMR chemical shifts in fluorine-containing proteins?. *J. Am. Chem. Soc. 122*, 4408–4417.

(44) Dubois, B. W., and Evers, A. S. (1992) F-19-NMR spin-spin relaxation (T_2) method for characterizing volatile anesthetic binding to proteins: Analysis of isoflurane binding to serum-albumin. *Biochemistry 31*, 7069–7076.

(45) Luz, Z., and Meiboom, S. (1963) Nuclear magnetic resonance study of protolysis of trimethylammonium ion in aqueous solution: Order of reaction with respect to solvent. *J. Chem. Phys. 39*, 366–369.

(46) Ahmed, A. H., Loh, A. P., Jane, D. E., and Oswald, R. E. (2007) Dynamics of the S1S2 glutamate binding domain of GluR2 measured using F-19 NMR spectroscopy. *J. Biol. Chem. 282*, 12773–12784.

(47) Anderluh, G., Razpotnik, A., Podlesek, Z., Macek, P., Separovic, F., and Norton, R. S. (2005) Interaction of the eukaryotic pore-forming cytolysin equinatoxin II with model membranes: F-19 NMR studies. *J. Mol. Biol. 347*, 27–39.

(48) Li, C. G., Lutz, E. A., Slade, K. M., Ruf, R. A. S., Wang, G. F., and Pielak, G. J. (2009) F-19 NMR Studies of α-synuclein conformation and fibrillation. *Biochemistry 48*, 8578–8584.

(49) Wang, G. F., Li, C. G., and Pielak, G. J. (2010) Probing the micelle-bound aggregation-prone state of α-synuclein with F-19 NMR apectroscopy. *ChemBioChem 11*, 1993–1996.

(50) Fukaya, T., and Ono, T. (2004) DFT-GIAO calculations of ^{19}F NMR chemical shifts for perfluoro compounds. *J. Comput. Chem. 25*, 51–60.

(51) Liu, Z., and Goddard, J. D. (2009) Predictions of the fluorine NMR chemical shifts of perfluorinated carboxylic acids, $C_nF_{2n+1}COOH$ (n = 6−8). *J. Phys. Chem. A 113*, 13921–13931.